Squeezed states and quantum chaos

K. N. Alekseev*) and D. S. Priĭmak

L. V. Kirenskiĭ Institute of Physics, Siberian Branch of the Russian Academy of Sciences, 660036 Krasnoyarsk, Russia

(Submitted 20 May 1997)
Zh. Éksp. Teor. Fiz. **113**, 111–127 (January 1998)

We examine the dynamics of a wave packet that initially corresponds to a coherent state in the model of a quantum rotator excited by a periodic sequence of kicks. This model is the main model of quantum chaos and allows for a transition from regular behavior to chaotic in the classical limit. By doing a numerical experiment we study the generation of squeezed states in quasiclassical conditions and in a time interval when quantum–classical correspondence is well-defined. We find that the degree of squeezing depends on the degree of local instability in the system and increases with the Chirikov classical stochasticity parameter. We also discuss the dependence of the degree of squeezing on the initial width of the packet, the problem of stability and observability of squeezed states in the transition to quantum chaos, and the dynamics of disintegration of wave packets in quantum chaos. © *1998 American Institute of Physics*. [S1063-7761(98)00801-4]

1. INTRODUCTION

At present the problem of generating squeezed quantum states draws a lot of attention, both from the standpoint of both pure knowledge and possible applications.[1–3] Most often the topic is squeezed states of the electromagnetic field. If in the simplest case we take a single-mode quantum field, which is described by the creation and annihilation operator $a^\dagger$ and a, the variances of the quadrature field operators $a_1=a+a^\dagger$ and $a_2=-i(a-a^\dagger)$ satisfy the uncertainty relation $\Delta a_1 \Delta a_2 \geqslant 1$, where the equality holds for a coherent state or vacuum. Then, in these simple terms, a squeezed state is a state for which the variance of one of the quadrature components is less than unity. Quantum fluctuations, determined by the uncertainty relation, are represented diagrammatically in the $a_1 a_2$ plane of the quadrature components by a circle for a coherent state or by an ellipse for a squeezed state. In a more systematic description of squeezing, the quantum-noise ellipse is determined in terms of the projection onto the same plane of the horizontal section of the Wigner distribution function, which gives the quasiprobability distribution for measuring the quadratic field components.[3]

A typical situation in experiments in generation of squeezed states is one in which a large number of photons participate in a nonlinear interaction and the amplitude of quantum fluctuations is small compared to the mathematical expectations of the observables.[2,3] In this case the common approach in explaining squeezing is to use the semiclassical setting, where the Wigner quantum function is actually associated with a classical distribution function and instead of examining the dynamics of the quantum-noise ellipse one considers the evolution of the classical phase volume.[3,4]

For quite a long time it has been known that squeezing of light is amplified in systems close to the bifurcation point between two different dynamical regimes.[3–6] Buildup of squeezing in such conditions was considered, e.g., for the parametric interaction of light waves[5] and for the interaction of Rydberg atoms with an electromagnetic mode in a high-Q cavity in a dynamical regime close to the separatrix.[4,6]

The following simple argument is used to explain the buildup of squeezing near a bifurcation point: quantum fluctuations build up for the physical variable that is unstable near the threshold. As a result there is nothing to stop the strong squeezing of fluctuations of the conjugate variable since in a nondissipative system phase volume is conserved.[3]

It must be noted at this point that a number of researchers (see Refs. 3–6) studied the buildup of squeezing near the instability threshold in optical systems with only regular dynamics. However, it is well known that strong (exponential) deformation of the phase volume is one of the main manifestations of dynamical chaos in classical systems.[7] The physical reason for such strong deformations of the phase volume is the local instability of motion, which usually manifests itself within a wide range of values of the control parameter of the dynamical system and not near the bifurcation point. According to the correspondence principle, in the quasiclassical limit a quantum system must manifest the properties of a classical system. Thus, it is quite natural to expect buildup of squeezing in the transition to quantum chaos, too. On the other hand, in a quantum mechanical description we speak only of the dynamics of wave packets, whose center moves almost along a classical trajectory in the course of a certain time interval. Hence in the quasiclassical limit the strong deformations of the phase volume, which accompany the transition to chaos, must manifest themselves in squeezing along a certain direction up to the point when quantum effects produce strong smearing of the wave packet.

As far as we know, the generation of squeezed states in a system with chaotic dynamics was first examined in Refs. 8–10. By employing the $1/N$-expansion method[6,11] (here N is the number of quantum states participating in the dynamics of the system) it was found in Refs. 8 and 9 that the squeezing of light increases significantly in the transition to chaos during the time interval for which quantum–classical correspondence is well-defined.[12] This result was illustrated in Refs. 8 and 9 by the example of the generalized Janes–

Cummings model, which allows a transition from regular dynamics to chaotic dynamics in the classical limit.[13] Then this result was generalized to the case of arbitrary single-mode quantum-optical systems in Ref. 14. The squeezing of wave packets in quantum chaos was also briefly discussed in Ref. 10.

However, the main results of Refs. 8, 9 and 14 were obtained by using a form of perturbation theory (the $1/N$-expansion). In this connection it should be interesting to study the generation of squeezed states in the numerical solution of the Schrödinger equation proper for a simple quantum system that allows a transition to quantum chaos.

In the present paper we study the generation of squeezed states in the time evolution of an initially Gaussian wave packet in the model of a quantum rotator excited by a periodic sequence of kicks, called the kicked quantum rotator. The model was first introduced by Casati *et al.*[15] and at present is the main model in studies of quantum chaos (see, e.g., the review in Refs. 16–18). The quantum rotator model is attractive mainly for two reasons: first, the classical limit for this model is a well-studied standard map,[19] and second, in numerical calculations it is fairly easy to study the dynamics of the model in the quasiclassical region with a large number of quantum levels.

We examine the dynamics of narrow Gaussian packets in a rotator with 2^{17} ($\approx 10^5$) levels. We define squeezing for the generalized quadrature operator

$$X_\theta = a\ \exp(-i\theta) + a^\dagger \exp(i\theta),$$

where θ is a real parameter. It is this type of squeezing that is observed in the homodyne detecting scheme, where θ is determined by the phase of the reference beam.[1] We will see that as long as the wave packet is localized, the degree of squeezing correlates well with the degree of local instability in the system. Here the greater the instability, the stronger the squeezing achieved in a shorter time interval. Squeezing is much stronger in quantum chaos than it is in regular motion. We will also see that the narrower the initial wave packet, the higher the degree of squeezing that can be achieved. We attribute this to the fact that a narrow wave packet is closer in its evolution to the classical trajectory than a broad one, with the result that it is more sensitive to local instabilities in the motion, which leads to strong squeezing.

We will also consider the problem of stability and observability of squeezing in the transition to chaos. More precisely, we will study the time dependence of the optimum values of the phases θ of the generalized quadrature operator X_θ for which the squeezing is at its maximum (this is known as principal squeezing[20,21]). We will show that in strong chaos and in long time intervals the optimum values of the phases change dramatically even under a small perturbation of the parameters of the initial Gaussian packet. Such a squeezing regime is unstable and difficult to observe. On the other hand, our results suggest that in weak chaos squeezing is fairly stable.

We will also briefly discuss the dynamics of disintegration of wave packets in chaos. Here we will show that a typical scenario of disintegration of an initially localized wave packet in chaos consists of two stages: the initial spread of the packet, and the catastrophic disintegration of the packet into many small subpackets. Here our results agree on the whole with the results of Casati and Chirikov.[18]

Note that earlier the dynamics of narrow Gaussian packets in the quasiclassical region was studied numerically for the model of a quantum rotator with kicks,[22,23] and also the model of a kicked quantum top[24] and for the quantum-cat–Arnold model[25] in connection with the problem of quantum–classical correspondence in quantum chaos. However, in these papers the generation of squeezed states was not considered.

The model of a quantum rotator is extremely popular in theoretical studies of quantum chaos. On the other hand, recently possibilities of implementing variants of this model in optical systems have been discussed.[26] Moreover, the quantum rotator model has been realized in experiments in the interaction of laser light and cooled atoms.[27] Hence our results on the buildup of squeezing in the transition to quantum chaos in a rotator are also related to experimentally realizable systems.

The plan of this paper is as follows. In Sec. 2 we discuss the quantum map of the rotator model and find how to calculate principal squeezing. The method used in numerical calculations is developed in Sec. 3, and the main results in the dynamics of squeezing are given in Sec. 4. Finally, in Sec. 5 we draw the main conclusions and consider the possibility of verifying our results in experiments on squeezing buildup.

2. THE QUANTUM ROTATOR MODEL AND SQUEEZED STATES

Let us examined the model of a quantum rotator with periodic delta-function kicks. Here we follow the notation of Ref. 23. The Hamiltonian for such a model is

$$H = \frac{p^2}{2mL^2} - \delta_p(t/T)\, mL^2\omega_0^2 \cos x,$$

$$\delta_p(t/T) = \sum_{j=-\infty}^{+\infty} \delta(j - t/T), \tag{1}$$

where x is the cyclic variable with a period 2π, L is the characteristic size of the rotator, m is the rotator mass, and ω_0 is the frequency of linear vibrations. The function $\delta_p(t/T)$ describes a periodic sequence of kicks with a period T, where $\delta(x)$ is the Dirac delta function. Let us introduce new variables

$$\alpha = mL^2\omega_0^2 T, \quad \beta = \frac{T}{mL^2}, \tag{2}$$

and measure time in units of T, i.e., $t \to t/T$. Then the Schrödinger equation assumes the form

$$i\hbar \frac{\partial \Psi}{\partial t} = -\frac{\hbar^2\beta}{2} \frac{\partial^2 \Psi}{\partial x^2} - \delta_p(t)\,\alpha \cos x \cdot \Psi. \tag{3}$$

Due to the periodicity of $\Psi(x)$ in x the solution of Eq. (3) can be written as follows:

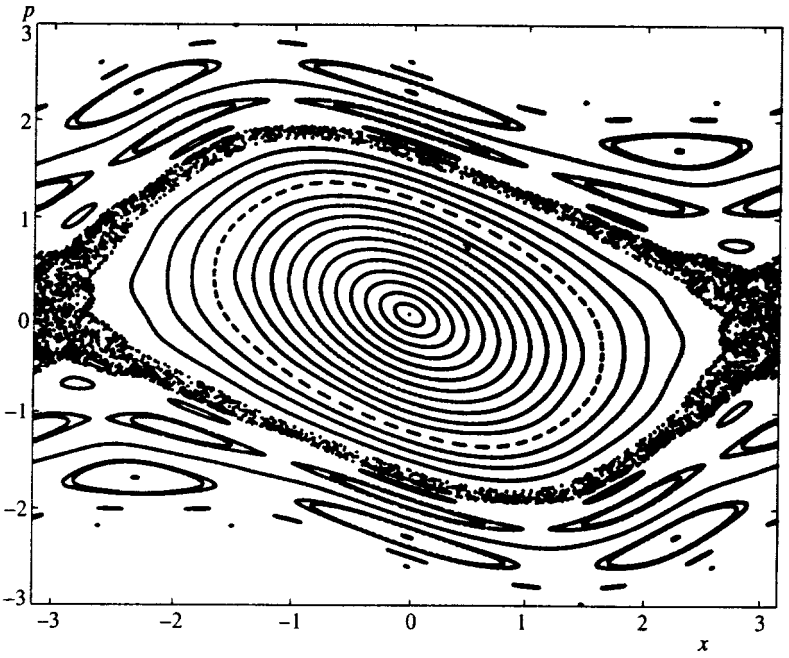

FIG. 1. Phase portrait of the classical standard map for $K=0.8$.

$$\Psi(x)=\frac{1}{\sqrt{2\pi}}\sum_{k=-\infty}^{+\infty}e^{ikx}A_k(t),$$

$$A_k(t)=\frac{1}{\sqrt{2\pi}}\int_0^{2\pi}\Psi(x)e^{-ikx}dx. \tag{4}$$

Using the standard procedure,[16,23] we obtain the quantum map in the form

$$\Psi_{n+1}=U_xU_p\Psi_n,$$

$$U_p=\exp\left(-\frac{i\beta}{2\hbar}\hat{p}^2\right),\quad U_x=\exp\left(\frac{i\alpha}{\hbar}\cos(\hat{x})\right), \tag{5}$$

where Ψ_n is the value of the wave function at the tome immediately after the nth kick. The time evolution of the wave function in the map (5) is determined solely by two parameters, $\alpha/\hbar$ and $\beta\hbar$. Since U_p is diagonalized in the p-representation, U_x is diagonalized in the x-representation, and the transition between x- and p-representations is given by the Fourier transformation (4), the map (5) actually reduces to

$$\Psi_{n+1}(x)=U_xF^{-1}U_pF\Psi_n(x), \tag{6}$$

where F and F^{-1} are the direct and inverse Fourier transforms.

Sometimes it proves useful to use the quantum map written in terms of the probability amplitudes A_k of transitions between the unperturbed levels of the rotator.[15] Combining (4) and (5), we obtain

$$A_k^{(n+1)}=\sum_{m=-\infty}^{+\infty}F_{km}A_m^{(n)},$$

$$F_{km}=(-i)^{k-m}\exp\left(-\frac{i\hbar\beta m^2}{2}\right)J_{k-m}\left(\frac{\alpha}{\hbar}\right), \tag{7}$$

where $J_l(z)$ is the Bessel function of order l and argument z, and the superscript (n) on the variable A stands for the number of the kick. Bearing in mind that the Bessel functions with $|l|\geqslant z$ rapidly decrease with increasing l, we see from (7) that, with exponential accuracy, in the course of a single kick $2\alpha\hbar^{-1}$ unperturbed rotator levels are captured. Below we consider the case where $\alpha/\hbar$ is large, which is typical of quantum chaos problems.

In the classical limit the Hamiltonian (1) reduces to the standard map

$$P_{n+1}=P_n-K\sin x_{n+1},\quad x_{n+1}=x_n+P_n\pmod{2\pi}, \tag{8}$$

where $P_n=\beta p_n$, with the subscript n denoting the values of x and P immediately after the nth kick, and $K\equiv\alpha\beta$ is the Chirikov parameter.[1)] Strong and global chaos sets in for $K>1$. For $K<1$ the larger part of the phase plane is filled with regular trajectories, although small regions with local chaos exist no matter how small K may be.[19] The phase portrait for the map (8) at $K=0.8$ is depicted in Fig. 1. The chaotic layer lies near the separatrix of the main resonance, which passes through the hyperbolic points $(\pm\pi,0)$. In our calculations we usually take a wave packet whose center of gravity lies near a hyperbolic point.

For the initial state of the quantum map (5) we take the Gaussian wave packet

$$\Psi(x)=(2\pi\sigma^2)^{-1/4}\exp\left(-\frac{(x-x_0)^2}{4\sigma^2}+ik_0(x-x_0)\right), \tag{9}$$

where

$$\langle x\rangle=x_0,\quad \langle\delta x^2\rangle\equiv\langle x^2\rangle-\langle x\rangle^2=\sigma^2,$$

$$p_0\equiv\langle p\rangle=\hbar k_0,\quad \langle\delta p^2\rangle=\hbar^2/4\sigma^2,$$

and k_0 is an integer. The packet is assumed narrow:

$$\sigma \ll x_0, \quad \langle \delta p^2 \rangle \ll \hbar k_0.$$

Note that in view of its periodicity in x the wave packet (9) is generally not a state that minimizes the uncertainty relation. But in the case of a narrow packet it is essentially indistinguishable from a minimum-uncertainty state.[22–24]

A typical initial quantum state in studies of light squeezing is a coherent state.[1–3] Such a state is an eigenfunction of the annihilation operator a, which in the present notation can be written as

$$a = \frac{1}{\sqrt{2\hbar}} \left(\sqrt{\gamma}\hat{x} + i \frac{\hat{p}}{\sqrt{\gamma}} \right), \quad \gamma = \left(\frac{\alpha}{\beta} \right)^{1/2}. \tag{10}$$

The fact that the annihilation operator has such an appearance can easily be understood if we consider the following limiting case of the harmonic oscillator that follows from (3):

$$i\hbar \frac{\partial \Psi}{\partial t} = -\frac{\hbar^2 \beta}{2} \frac{\partial^2 \Psi}{\partial x^2} + \frac{\alpha x^2}{2} \Psi. \tag{11}$$

Now we can show that the wave function (9) is a coherent state, i.e., an eigenfunction of (10), if we put

$$\sigma^2 = \frac{\hbar}{2\gamma}. \tag{12}$$

Let us now turn to the problem of squeezing.

In light squeezing experiments,[1] the observable quantity is the variance of the generalized quadrature operator

$$X_\theta = a e^{-i\theta} + a^\dagger e^{i\theta}, \tag{13}$$

where θ is the phase of the reference beam in the homodyne detecting scheme. In the particular cases where $\theta = 0$ or $\theta = \pi/2$ Eq. (13) yields the following expressions for the generalized position and momentum operators:

$$X_1 = a + a^\dagger, \quad X_2 = -i(a - a^\dagger), \quad [X_1, X_2] = 2i, \tag{14}$$

with the uncertainty relation $\langle \delta X_1^2 \rangle \langle \delta X_2^2 \rangle \geqslant 1$, where averaging is done over an arbitrary quantum state and equality is achieved for a coherent state. The standard definition of quadrature squeezing is the condition[1,3]

$$\min(\langle \delta X_1^2 \rangle, \langle \delta X_2^2 \rangle) < 1, \tag{15}$$

i.e., the variance of one of the quadrature components is smaller than for the coherent state.

In a more general case we consider the variance $\langle \delta X_\theta^2 \rangle$ of the operator (13), and the state is assumed squeezed if the value of $\langle \delta X_\theta^2 \rangle$ in this state for some value of θ is smaller than in the coherent state.[20,21] Experiments actually determine the minimum S of this variance as a function of the angle θ:

$$S = \min_{\theta \in [0, 2\pi]} \langle \delta X_\theta^2 \rangle. \tag{16}$$

Using the definition (13) of X_θ, we can show[20,21] that

$$S = 1 + 2\langle \delta a^\dagger \delta a \rangle - 2\sqrt{\langle \delta a^2 \rangle \langle \delta a^{\dagger 2} \rangle}, \tag{17}$$

and the minimum of $\langle \delta X_\theta^2 \rangle$ is reached at an optimum phase value $\theta = \theta^*$ defined as follows:[21]

$$e^{2i\theta^*} = -\sqrt{\frac{\langle \delta a^2 \rangle}{\langle \delta a^{\dagger 2} \rangle}}. \tag{18}$$

For our discussion it is convenient to express S in terms of the cumulants of the operators x and p. Using the definition (10) of operator a and Eq. (17), we obtain

$$S = \frac{1}{\hbar} \left(\frac{\langle \delta p^2 \rangle}{\gamma} + \langle \delta x^2 \rangle \gamma - \sqrt{(\langle \delta x^2 \rangle \gamma - \langle \delta p^2 \rangle / \gamma)^2 + 4c^2} \right), \tag{19}$$

where

$$c = \tfrac{1}{2}(\langle (xp + px) \rangle - 2\langle x \rangle \langle p \rangle).$$

Clearly each Gaussian packet satisfies $S = \hbar / 2\sigma^2 \gamma$, while for a coherent state we have, in view of (12), $S = 1$. Hence a state is squeezed if

$$S < 1. \tag{20}$$

The condition determines the principal squeezing attainable in homodyne detecting.[20]

The maximum of the variance $\langle \delta X_\theta^2 \rangle$ in θ can be defined in the same way the minimum was defined in (16). We denote it by $\overline{S}$. Then we can show that the dependence of $\overline{S}$ on the cumulants differs from (19) only in the sign in front of the square root, so that we have

$$S\overline{S} \geqslant 1. \tag{21}$$

Thus, squeezing in S (Eq. (20)) is accompanied by dilation in $\overline{S}$.

Note that in contrast to the quadrature squeezing (15), the definition (19) of principal squeezing contains quadrature correlators of the $\langle xp \rangle$ type. This is very important for systems with discrete time, to which the model of a quantum rotator excited by kicks belongs. The thing is that the quadrature squeezing (15) is essentially unobservable in such systems, although the principal squeezing (19) and (20) may occur.[2)] In Sec. 4 we discuss the time dependence of S.

3. THE NUMERICAL METHOD

Several features of the numerical method must be mentioned. The interval in x from 0 to 2π is partitioned into N segments $\Delta x = 2\pi/N$, and the wave function $\Psi(x)$ is represented by a discrete sequence of values (column vector $|\Psi\rangle$) of length N, so that $\Psi_l = \Psi(l\Delta x)$, $l \in [0,1,\cdots, N-1]$. Accordingly, in the sum in (4) k varies from 0 to $N-1$. In our numerical method N is an integral power of two. Here the operator F in (6) is interpreted as the fast Fourier transform, which induces the following transformations:

$$F\colon \Psi_l \to A_k, \quad F^{-1}\colon A_k \to \Psi_l. \tag{22}$$

To determine the principal squeezing, we must calculate $\langle \delta q^2 \rangle$, $\langle \delta p^2 \rangle$, and $\langle xp \rangle$ (see Eq. (19)). For instance, the calculation of $\langle xp \rangle$ proceeds along the following lines:

$$\langle xp \rangle = \langle \Psi | \mathbf{x} F^{-1} \mathbf{p} F | \Psi \rangle,$$

where $\langle\Psi|$ is obtained by transposing the vector $|\Psi\rangle$ and then finding the complex conjugate of the result, while $\mathbf{x}$ and $\mathbf{p}$ are vectors that initially have the form

$$\mathbf{x}=[0,\ \Delta x,\ 2\Delta x,\cdots,\ 2\pi-\Delta x],$$

$$\mathbf{p}=[0,\ 1,\ 2,\cdots,\ N-1].$$

The fact that x is defined modulo 2π requires following the wave packet and ensuring that it is defined correctly during the passage through the end-points of the interval $[0,\ 2\pi]$. We set up the process in the following manner. When the center of the wave packet in the x-representation approaches an edge of the half-interval $[0,\ 2\pi]$, the wave function $\Psi(x)$ is examined on a new interval, $[-\pi,\pi]$, with a new vector

$$\mathbf{x}=[0,\Delta x,\cdots,\pi,-\pi+\Delta x,-\pi+2\Delta x,\cdots,-2\Delta x,-\Delta x],$$

since $(-k\Delta x)\bmod 2\pi=(2\pi-k\Delta x)\bmod 2\pi$, where k is an integer. The transition from $[-\pi,\pi]$ to $[0,2\pi]$ is treated similarly.

Calculations in the p-representation have their own special features. For instance, although for the Hamiltonian (1) the momentum is defined in the interval from $-\infty$ to $+\infty$, in numerical calculations we deal only with a finite range of values of momentum p, a range specified by the number N of Fourier transforms in the expansion (4). To avoid the possible problem of reflection of the wave packet from an edge of the given interval in the p-representation,[3)] we select this interval in each iteration of map (6) in such a way that the maximum of the absolute value of the wave function of the packet is always at the center of the given interval (actually, we renumber the vector $\mathbf{p}$).

The process of calculating the next iteration of the quantum map (6) is terminated as soon as the packet ceases to be sufficiently localized either in the x-representation or in the p-representation, i.e., when the number of Fourier transforms actually involved in the calculation process is smaller than needed. We write the conditions for packet delocalization mentioned earlier. To this end we introduce the notation

$$\xi=\max_{[0,2\pi]}|\Psi(x)|,\quad \chi=\max\{|A_1|,|A_2|,\cdots,|A_N|\},$$

and A_{left} and A_{right} are the values of A_k belonging, respectively, to the left and right edges of the finite interval in which the wave function in momentum space, the finiteness being due to the finite number N of Fourier transforms in the expansion (4). The calculation is terminated when one of the two inequalities,

$$\max\left\{\frac{|A_{\text{left}}|}{\chi},\frac{|A_{\text{right}}|}{\chi}\right\}>\varepsilon\quad\text{or}\quad\frac{|\Psi(z)|}{\xi}>\varepsilon,$$

is valid (here $z=0$ if $x\in[0,2\pi]$ or $z=\pi$ if $x\in[-\pi,\pi]$. In this paper we used the value $\varepsilon=0.002$).

4. THE MAIN RESULTS

For the initial wave function in our calculations we took the coherent state (a Gaussian wave packet) with $\hbar=10^{-6}$ and $k_0=10\,000$, and σ was varied between 0.04 and 0.07. We fixed the initial width σ of the wave packet and the Chirikov parameter K, in terms of which the parameters α and β in the evolution operator (5) are expressed as follows:

$$\alpha=K^{1/2}\frac{\hbar}{2\sigma^2},\quad \beta=K^{1/2}\frac{2\sigma^2}{\hbar}. \tag{23}$$

These formulas are obtained by combining the definition $K=\alpha\beta$ and Eqs. (10) and (12).

In Sec. 2 we found that the number of unperturbed-rotator levels captured in one kick is roughly $2\alpha/\hbar$. From (23) it follows that in our case this number is $K^{1/2}/\sigma^2$ and amounts to several tens of thousands for the adopted widths σ of the wave packet.

In our calculations K was varied between 0.2 and 2 with a step of 0.02. We found the time dependence of the squeezing S (19) and the optimum value of the phase θ^* at which $\langle\delta X_\theta^2\rangle$ is at its minimum. To demonstrate the correlation that exists between the degree of squeezing and the chaos characteristics[9,14] we calculated

$$d=[\langle\delta x^2\rangle+\langle\delta p^2\rangle]^{1/2}. \tag{24}$$

It can be shown[9,14,28] that in the classical limit and while the wave packet is well-localized, i.e., $[\langle\delta x^2\rangle]^{1/2}\ll x_0$ and $[\langle\delta p^2\rangle]^{1/2}\ll p_0$, the d of (24) corresponds to the following separation in phase space:

$$d_{\text{cl}}(t)=[(\Delta x)^2+(\Delta p)^2]^{1/2}, \tag{25}$$

where $(\Delta x(t),\ \Delta p(t))$ is the solution of the linear small-perturbation equations near the classical trajectory $(x(t),\ p(t))$. The quantity $d_{\text{cl}}(t)$ characterizes the divergence of two initially close trajectories and enters into the definition of the largest classical Lyapunov exponent

$$\lambda=\lim_{t\to\infty}\frac{d_{\text{cl}}(t)}{t}. \tag{26}$$

For a classical standard map with strong chaos $K\gg 1$ we have the simple dependence $\lambda\approx\ln(K/2)$ (see Ref. 19). The Lyapunov exponent (26) is an asymptotic characteristic of chaos. For finite time intervals[7]

$$d_{\text{cl}}(t)\approx\exp(h(x,p)t), \tag{27}$$

where the exponent h is a function of a point in phase space and coincides, in order of magnitude, with the Lyapunov exponent λ, but in some time intervals the difference between the two may be significant. The latter fact can be explained by the strong inhomogeneity in the statistical properties of the phase space of chaotic systems and, correspondingly, by the different rates of divergence of trajectories in different regions of phase space through which the system passes in its time evolution. It must be noted at this point that the dependence of h on the parameter K is extremely complicated. What is important, however, is only the property of the strong (exponential) increase of d_{cl} specified by (27) in the presence of chaos, a property often called local instability.[7] When the motion is regular, the time dependence of d_{cl} is much weaker—it follows a power function.[7]

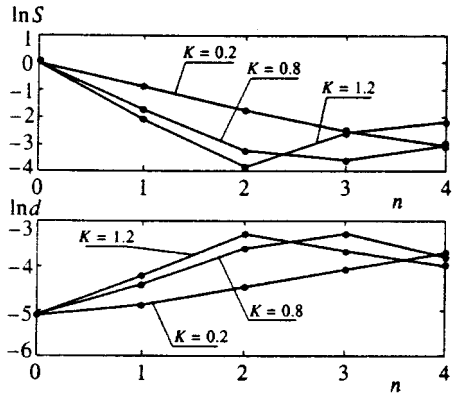

FIG. 2. Time dependence of the logarithm of squeezing S (the upper part of the figure) and $\ln d$ defined in Eq. (24) (the lower half of the figure); $x_0=\pi$ and $\sigma=0.006$.

On the other hand, it is h that determines the rate of phase-volume deformation: the stronger the local instability, the greater the phase-volume deformation in a given time interval.

Since in our case quantum–classical correspondence and the concept of chaos are well-defined only in a very short time interval, while the wave packet remains localized, it is meaningful to consider the correlations existing between the time dependence of the squeezing and that of the quantity d (see (24)), which in the classical limit becomes $d_{\rm cl}$ (see (25)).

Figure 2 depicts the time dependence of the logarithm of squeezing S and $\ln d$ for different values of K, when the center of gravity is of the wave packet is initially at the point $x_0=\pi$, $p_0=\hbar k_0=0.01$. This initial condition is close to a hyperbolic point through which the chaotic layer passes even when K is small (see Fig. 1). Figure 2 shows that the larger the squeezing (the smaller the value of S) the larger the local instability (the larger the values of $\ln d$) up to $n\approx 4$, when the packet spread becomes so large that purely quantum effects become important.

For another initial condition, $x_0=\pi/2$ and $p_0=0.01$, which is closer to an elliptic point and hence lands in the chaotic region only at large values of K, the dynamics of squeezing is depicted in Fig. 3. We see that in this case squeezing is stronger by a factor of almost two than under the conditions of Fig. 2 in the same time interval. On the other hand, both Fig. 2 and Fig. 3 exhibit an increase in squeezing as a function of the parameter K, which controls the development of chaos in the system.

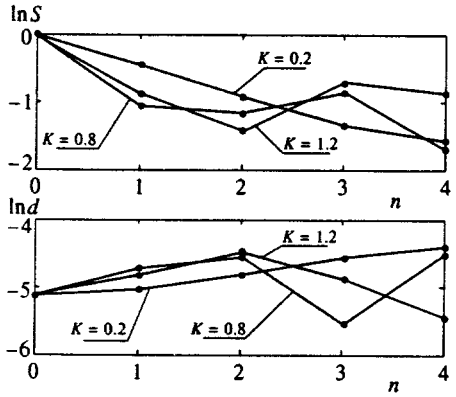

FIG. 3. The same as in Fig. 2 but for $x_0=\pi/2$.

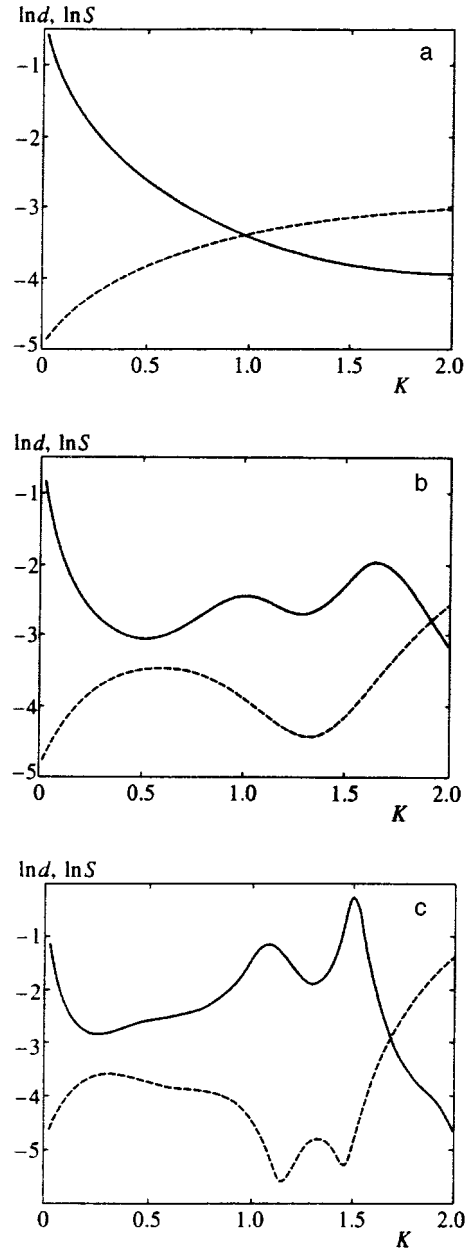

FIG. 4. Logarithm of the squeezing S (solid curves) and $\ln d$ (dashed curves) as functions of the Chirikov parameter K for a fixed number of kicks: (a) $n=3$, (b) $n=4$, and (c) $n=5$; $x_0=\pi$ and $\sigma=0.007$.

Let us study the correlation between squeezing and the degree of local instability in the system for different values of K in greater detail. The K-dependence of the degree of squeezing calculated after a fixed number of kicks at $x_0=\pi$ and $p_0=0.01$ is depicted in Fig. 4. After the third kick the correlation between $\ln S$ and $\ln d$ become very evident (Fig. 4a). However, small discrepancies in this dependence may appear as the number of kicks grows. Such discrepancies become evident, for instance, after the fourth kick for $1.1\lesssim K\lesssim 1.4$ (Fig. 4b). After five kicks, $n=5$, the correlation between $\ln S$ and $\ln d$ is restored (Fig. 4c). Note that this

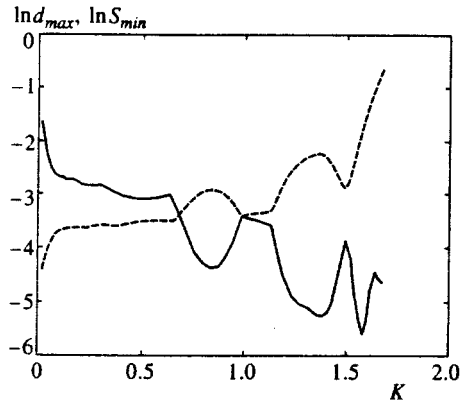

FIG. 5. Logarithm of the minimum squeezing $S_{\min}$ (solid curves) and of the local instability $d_{\max}$ (dashed curves) as functions of the Chirikov parameter K after seven kicks. The parameters and initial conditions are the same as in Fig. 4.

behavior pattern is quite typical. Hence, to establish the correlation between local instability and squeezing more clearly, a certain procedure of coarsening (averaging) these quantities in the given time interval is needed. In our study we determine the minimum squeezing $S_{\min}$ in a time interval during which the packet remains well-localized for most values of K considered here, and hence the maximum $d_{\max}$ in the same time interval. We found that there is a distinct correlation between $S_{\min}$ and $d_{\max}$: the larger the value of $d_{\max}$ the smaller the value of $S_{\min}$, and vice versa. An example of such a dependence is depicted in Fig. 5, where $S_{\min}$ and $d_{\max}$ were calculated after six kicks. Note that the diagrams do not go farther than $K>1.7$ because after six kicks the wave packet becomes delocalized for $K>1.7$ and calculating averages and local instability becomes meaningless.

We also studied the dependence of the dynamics of squeezing on the initial width σ of the wave packet. The results are depicted in Fig. 6. Clearly, the narrower the packet the stronger the squeezing achieved in a fixed time interval. This dependence arises because a narrow wave packet travels farther along its classical trajectory than a wide packet, so that it undergoes stronger deformations related to nonlinear classical dynamics. The exponential decrease is replaced by growth when the wave packet departs from the classical limit and the dynamics is of an essentially quantum nature.

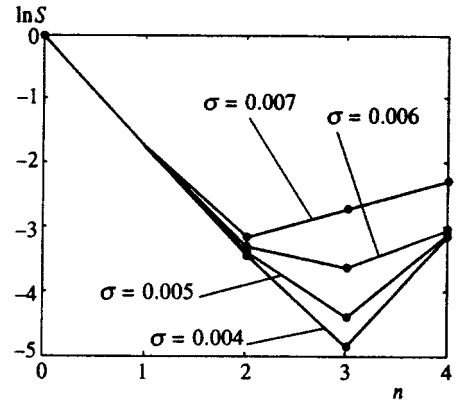

FIG. 6. Time dependence of the logarithm of squeezing S for different initial widths σ of the wave packet at fixed $K=0.8$; $x_0=\pi$.

Now let us examine the problem of stability and observability of squeezing in chaos. The figures mentioned earlier can serve to illustrate the statement that the stronger the chaos the stronger the principal squeezing. However, the definition (19) of principal squeezing is related to fixing the phase, $\theta=\theta^*$. Here θ^* is time-dependent even for exactly integrable systems.[21] When chaos is strong, the time dependence of $\theta^*(t)$ in the classical limit may be extremely complicated. Indeed, in addition to dilation and squeezing, the main feature of chaos in classical systems with a bounded phase space is the multiple formation of folds of the phase volume as chaos evolves.[7] Hence the process of finding the ''minimum width'' of a phase drop, which actually amounts to finding the θ^* vs. t dependence in the quasiclassical limit, becomes unstable for large time intervals.

Basing our reasoning on a similar semiclassical picture, we examined the stability of the time dependence of the optimum phase $\theta^*(t)$ calculated quantum mechanically with a small perturbation of the initial position of the wave packet. More precisely, we found the time dependence of the optimum phase θ_1^* with the initial condition $x_0=\pi$ and, similarly, $\theta_2^*(t)$ with the initial condition $x_0=\pi-0.05$. We denote the difference of these phases by

$$D(t)=\theta_1^*(t)-\theta_2^*(t).$$

Since θ^* is periodic with a period π (see Eq. (18)), it is natural to take $\sin 2D$ as the quantity of interest, since in this way we avoid breaks in the diagrams related to the periodicity of θ^*. The dependence of $\sin 2D$ on the Chirikov parameter K for different fixed numbers of kicks is depicted in Figs. 7a–7c. After two kicks (Fig. 7a) the maximum value of $|\sin 2D|$ does not exceed 0.035 at $K=2$. After three kicks (Fig. 7b) the value of D becomes significant at $K\gtrsim 1.2$. Finally, after four kicks (Fig. 7c) the process of measuring squeezing becomes essentially unstable at $K\gtrsim 1$. Indeed, in these condition with a small perturbation of the initial position of the wave packet, the difference of the optimum phases reaches a value of order π. In Ref. 9 such generation of squeezed states was called unstable squeezing. As Fig. 7 implies, unstable squeezing is observed when chaos is strong and the time intervals are such that semiclassical description is valid. On the other hand, for short time intervals and small K's the squeezing is strong and stable.

To conclude this section we will briefly touch on the problem of the dynamics of disintegration of coherent states in chaos, a problem that is of interest by itself. Figures 8a and 8b depict the dependence of $|\Psi|$ on x and of $|A_k|$ on k (see Eq. (4)). Actually, Fig. 8 gives the shape of the wave function in the coordinate and momentum representations for an initially narrow wave packet with $[\langle \delta x^2\rangle]^{1/2}(t=0)\equiv\sigma=0.006$ and $[\langle \delta p^2\rangle]^{1/2}(t=0)=\frac{1}{12}\times 10^{-3}$. The relatively small value $K=1.2$ makes it possible to examine the fairly long evolution of the wave packet up to the point of its total disintegration.[4)] After six kicks (Fig. 8a) the wave packet spreads out significantly, but on the whole retains its bell-shaped structure. What follows is a

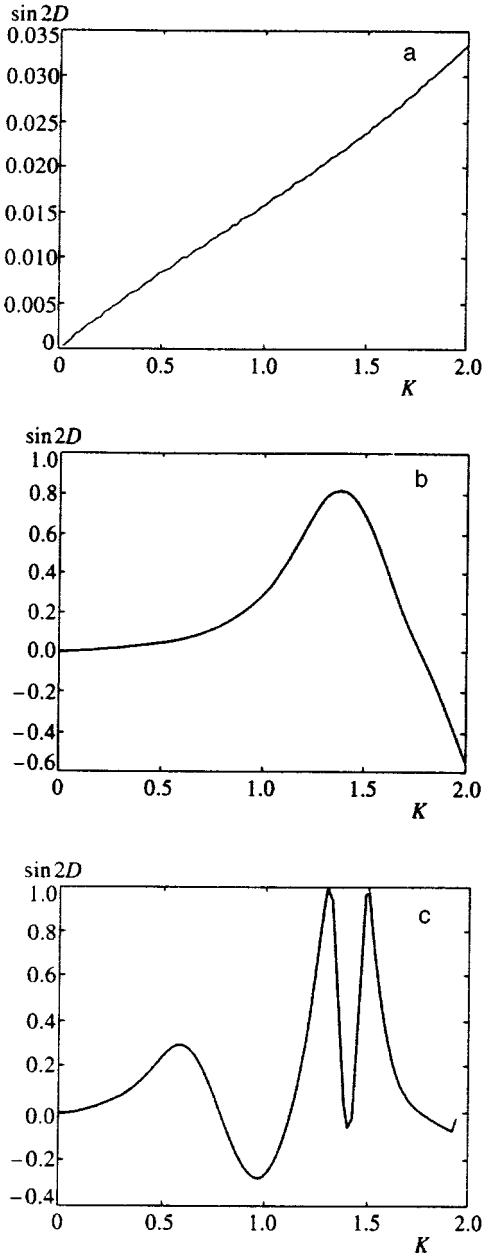

FIG. 7. The difference D of optimum phases as a function of the parameter K at $\sigma=0.006$, $x_0=\pi$, and a fixed number of kicks: (a) $n=2$, (b) $n=3$, and (c) $n=4$.

disintegration of the packet into many small packets, with the characteristic shape of the wave function depicted in Fig. 8b (after 18 kicks). Finally, very soon the wave function becomes so dissected that even 2^{17} Fourier harmonics are insufficient to describe the evolution correctly (for the data of Fig. 8 this happens approximately at the 20th kick). Qualitatively, the same pattern of the evolution of the wave packet was observed at higher values of K: first the broadening, or ''swelling,'' of the wave packet, and then its rapid disintegration into many very small subpackets. The differences in packet disintegration for large values of K in comparison with the case $K\simeq 1$ (Fig. 8) boil down to two facts: first, the swelling of the packet and the disintegration occur very rapidly (it takes only several kicks to complete the process), and second, the emerging subpackets are extremely small. Hence the process of disintegration of wave packets in strong chaos resembles an explosion. On the whole, the pattern being described agrees well with the pattern obtained from the analysis of the behavior of the Wigner function,[18] although we observed some anomalies. In particular, for fairly narrow wave packets ($\sigma=4\times10^{-3}$) we observed the disintegration of the initial packet into two fairly large subpackets. Ripples then appeared on the subpackets, and the two disintegrated into many small packets.

A more detailed description of the disintegration of coherent states in chaos requires further investigations.

5. DISCUSSION AND CONCLUSION

Thus, in this work we have used a numerical experiment to study the dynamics of generation of squeezed states in the evolution of a Gaussian packet in the quasiclassical limit for the model of a quantum rotator excited by kicks. We show that within the time interval where the packet is well-localized the squeezing becomes stronger in the transition to chaos. For strong chaos and in long time intervals the squeezing process becomes unstable. These results, obtained through direct numerical simulation, are in good agreement with the results obtained by perturbation-theoretic techniques and for other models.[8,9,14]

In the final stages of preparing the manuscript for press we became acquainted with two recent papers[29] also devoted to the problem of generating nonclassical states (squeezing and antibunching) in quantum chaos. Rui-Hue Xie and Gong-ou Xu[29] presented the results of numerical experiments on the dynamics of quadrature squeezing in simple quantum models that allow a transition to chaos in the classical limit: the Lipkin–Meshkov–Glick model[30] and the Belobrov–Zaslavskiĭ–Tartakovskiĭ model.[31] In contrast to our approach, Rui-Hue Xie and Gong-ou Xu[29] were interested in the long-time limit, when the wave packets are delocalized and this sense the quantum–classical correspondence is completely violated. They found that quadrature squeezing disappears in the transition to quantum chaos, although to some degree squeezing is always present in regular motion. It must be noted at this point that Rui-Hue Xie and Gong-ou Xu[29] noticed the existence of nonzero squeezing of some sort in the short-time limit and for quantum chaos, but they did not observe the buildup of squeezing described in the present paper, probably because in their numerical experiments[29] the quasiclassicality parameter was not sufficiently large: only several hundred quantum levels participated in the dynamics of the system. Thus, their results do not contradict ours and augment them in another limiting case, the limit of long times of motion. The description of the dynamics of squeezing in the case intermediate between the one described in the present paper and the one studied in Ref. 29 merits a separate investigation.

In conclusion we would like to make several remarks concerning the possibility of experimentally observing squeezing in quantum chaos on a time scale corresponding to a well-defined quantum–classical correspondence. At present essentially all squeezed-light experiments are done in the stationary regime. Squeezing in the transition to quantum

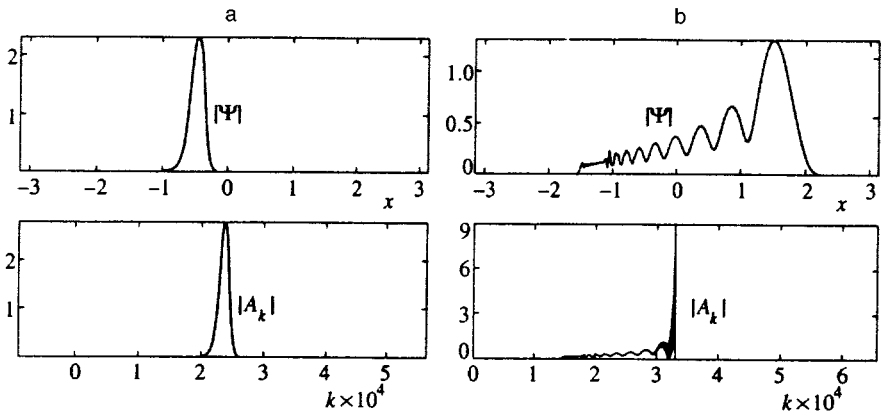

FIG. 8. Dependence of the absolute value of the wave function, $|\Psi|$ on x and dependence of the absolute value of the Fourier transforms, $|A_k|$, on k in the expansion (4) of the wave function at (a) $n=6$ and (b) $n=18$ and fixed $\sigma=0.006$, $K=1.2$, and $x_0=\pi$.

chaos builds up only over finite time intervals and in this sense is a transient dynamical phenomenon. The first experiments in light squeezing in transient regimes are only in the preliminary stage.[32] We hope that the development of effective experimental methods for observing squeezed states of light in transient dynamical regimes will also make it possible to observe the buildup of squeezing in the transition to quantum chaos.

On the other, as noted in the Introduction, it is much simpler to realized the quantum rotator model with kicks in atomic optics.[27] Moreover, it is much simpler to observe transient dynamical regimes in experiments with cooled atoms. Hence we believe that atomic-optics systems of the type discussed in Ref. 27 have great potential for observations of squeezed states in quantum chaos.

We are grateful to Claude Fabre, Jarmo Hietarinta, Zdenek Hradil, Juhani Kurkijärvi, Feodor Kusmartsev, Vlasta Peřinova, and Sergeĭ Turovets for stimulating discussions in stating the problem of squeezing and quantum chaos. We are also grateful to Andreĭ Kolovskiĭ and Jan Peřina for discussions and support at all stages of our work, and to Boris Chirikov for discussing the results and drawing our attention to his paper.[10] Preliminary investigation were done during the visit of one of the authors (K.N.A) to the Department of Physics, University of Illinois at Urbana-Champaign. K.N.A. is grateful to Prof. David Campbell for his hospitality. Partial support for this work was provided by the Russian Fund for Fundamental Research (Grant No. 96-02-16564a), the Krasnoyarsk Regional Scientific Fund (Grant No. 6F0030), INTAS (Grant No. 94-2058), and NATO (Linkage Grant No. 93-1602).

*)E-mail: kna@iph.krasnoyarsk.su

1)The unusual form of the standard map (8) is due to the fact that we find it convenient to take the values of x and p immediately after the nth kick rather than before the nth kick, as is done by the majority of researchers. It must be noted, however, that the properties of the standard map are retained.

2)Note that Lan[23] studied the time dependence of $\langle \delta a^2 \rangle$ and $\langle \delta p^2 \rangle$ for a quantum rotator on a time scale on which quantum–classical correspondence holds (Table I in Ref. 23). Both variances increase uniformly, so that quadrature squeezing (15) is impossible.

3)For a discussion of the problem of reflection and splitting of a wave packet due to the finite range of momentum in the close model of the quantum Arnold cat see Ref. 25.

4)In conducting numerical experiments in the dynamics of the disintegration of wave packets we did not use the procedure (described in Sec. 3) of terminating the counting process when the wave function becomes delocalized.

[1] D. F. Smirnov and A. S. Troshin, Usp. Fiz. Nauk **153**, 233 (1987) [Sov. Phys. Usp. **30**, 851 (1987)]; M. C. Teich and B. E. A. Saleh, Phys. Today **43**, No. 6, 26 (1990).
[2] S. Reynaud, A. Heidmann, E. Giacobino, and C. Fabre, in *Progress in Optics*, Vol. 30, E. Wolf (ed.), North-Holland, Amsterdam (1992), p. 1.
[3] C. Fabre, Phys. Rep. **219**, 215 (1992).
[4] A. Heidmann, J. M. Raimond, and S. Reynaud, Phys. Rev. Lett. **54**, 326 (1985).
[5] L. A. Lugiato, P. Galatola, and L. M. Narducci, Opt. Commun. **76**, 276 (1990).
[6] A. Heidmann, J. M. Raimond, S. Reynaud, and N. Zagury, Opt. Commun. **54**, 189 (1985).
[7] R. Z. Sagdeev, D. A. Usilov, and G. M. Zaslavskiĭ, *Nonlinear Physics: From the Pendulum to Turbulence and Chaos*, Harwood Academic, New York (1988).
[8] K. N. Alekseev, Preprint Kirensky Institute of Physics 674F, Krasnoyarsk (1991).
[9] K. N. Alekseev, Opt. Commun. **116**, 468 (1995).
[10] B. V. Chirikov, in Proceedings of the Second International Workshop on Squeezed States and Uncertainty Relations, Moscow, May 25–29, 1992, NASA Conference Publication 3219, 317 (1993).
[11] L. G. Yaffe, Rev. Mod. Phys. **54**, 407 (1982).
[12] G. P. Berman and G. M. Zaslavsky, Physica A **91**, 450 (1978); M. Berry, N. Balazs, M. Tabor, and A. Voros, Ann. Phys. (N.Y.) **122**, 26 (1979).
[13] K. N. Alekseev and G. P. Berman, Zh. Éksp. Teor. Fiz. **94**, No. 9, 49 (1988) [Sov. Phys. JETP **67**, 1762 (1988)]; **105**, 555 (1994) [**78**, 296 (1994)].
[14] K. N. Alekseev and J. Peřina, Phys. Lett. **231**, 373 (1997); submitted to Phys. Rev. E (1998).
[15] G. Casati, B. V. Chirikov, J. Ford, and F. M. Izrailev, in *Stochastic Behavior in Classical and Quantum Hamiltonian Systems*, G. Casati and J. Ford (eds.), Springer, Berlin (1979), p. 334.
[16] B. V. Chirikov, F. M. Izrailev, and D. L. Shepelyansky, Sov. Sci. Rev. C **2**, 209 (1981).
[17] *Chaos and Quantum Physics*, M. J. Giannoni, A. Voros, and J. Zinn-Justin (Eds.), Les Houches Session *LIL* 1989, Elsevier, Amsterdam (1991).
[18] G. Casati and B. V. Chirikov, Physica D **86**, 220 (1995).
[19] B. V. Chirikov, Phys. Rep. **52**, 263 (1979).
[20] A. Lukš, V. Peřinova, and J. Peřina, Opt. Commun. **67**, 149 (1988).
[21] R. Tanaś, A. Miranowicz, and S. Kielich, Phys. Rev. A **43**, 4041 (1991).
[22] R. F. Fox and B. L. Lan, Phys. Rev. A **41**, 2952 (1990); B. L. Lan and R. F. Fox, Phys. Rev. A **43**, 646 (1991); R. F. Fox and T. C. Elston, Phys. Rev. E **49**, 3683 (1994).
[23] B. L. Lan, Phys. Rev. E **50**, 764 (1994).
[24] R. F. Fox and T. C. Elston, Phys. Rev. E **50**, 2553 (1994).

[25] T. C. Elston and R. F. Fox, Preprint Georgia Inst. of Technol. (1994).
[26] J. Krug, Phys. Rev. Lett. **59**, 2133 (1987); R. E. Prange and S. Fishman, Phys. Rev. Lett. **63**, 704 (1989).
[27] F. L. Moore, J. C. Robinson, C. Bharucha, P. E. Williams, and M. G. Raizen, Phys. Rev. Lett. **73**, 2974 (1994); F. L. Moore, J. C. Robinson, C. F. Bharucha, B. Sundaram, and M. G. Raizen, Phys. Rev. Lett. **75**, 598 (1995).
[28] B. Sundaram and P. W. Milonni, Phys. Rev. E **51**, 1971 (1995).
[29] Rui-Hue Xie and Gong-ou Xu, Phys. Rev. E **54**, 1402 (1996); **54**, 2132 (1996).
[30] H. J. Lipkin, N. Meshkov, and A. J. Glick, Nucl. Phys. **62**, 188 (1965).
[31] P. I. Belobrov, G. M. Zaslavskiĭ, and G. Kh. Tartakovskiĭ, Zh. Éksp. Teor. Fiz. **71**, 1799 (1976) [Sov. Phys. JETP **44**, 945 (1976)].
[32] Claude Fabre, Université P. et M. Curie, Paris, France (private communication).

Translated by Eugene Yankovsky